A Parametric, Preliminary Structural Analysis and Optimization Approach with Manufacturing Cost Considerations

Mario A. Lee[1], Johanna Ceisel[2], Zhimin Liu[3], and Dimitri N. Mavris[4]
Georgia Institute of Technology, Atlanta, Georgia, 30332-0150

This paper briefly describes an approach that uses preliminary design methods and commercially available software to facilitate a coupling between structural design and manufacturing cost estimation at the preliminary design level. The approach is illustrated through a case study that features the structural analysis, optimization and manufacturing cost assessment of a sub-sonic fighter wing-box. An automated, parametric modeling and simulation environment is built and then used to provide the data required for the creation of surrogate models as functions of high level wing geometry and performance variables. These surrogate models are then used with a multi-objective genetic algorithm for the purpose of providing a family of non-dominated designs that facilitate a trade-off between weight and manufacturing cost. The approach is then generalized for application to other assemblies within the airframe.

Nomenclature

C_{lb}	=	section lift coefficient for basic lift distribution
C_{la1}	=	section lift coefficient for additional lift distribution at a wing lift coefficient of unity
c	=	local chord of wing
ε	=	angle of twist, degrees
$\bar{\varepsilon}$	=	average angle of twist, degrees
a	=	three dimensional lift slope per degree
A	=	aspect ratio
b	=	wing span
y	=	span-wise coordinate
Λ	=	sweep angle of wing quarter-chord line, degrees
ϑ	=	edge-velocity factor for symmetrical lift distributions
N_x, N_y	=	resultant, cross-sectional axial loads in the x and y directions, respectively
N_{xy}	=	resultant, cross-sectional in-plane shear load
M_x, M_y	=	resultant, cross-sectional bending moments about the y and x axes, respectively
M_{xy}	=	resultant, cross-sectional twisting moment
$\varepsilon_x, \varepsilon_y$	=	strains in the x and y directions, respectively
ε_{xy}	=	in plane shear strain
$\kappa_x, \kappa_y, \kappa_{xy}$	=	mid-surface curvatures
A	=	extensional stiffness matrix
B	=	coupling stiffness matrix
D	=	bending stiffness matrix

---

[1] Graduate Research Assistant, Aerospace Systems Design Laboratory, Daniel Guggenheim School of Aerospace Engineering, Student Member AIAA.

[2] Research Engineer II, Aerospace Systems Design Laboratory, Daniel Guggenheim School of Aerospace Engineering, Senior Member AIAA.

[3] Research Engineer II, Aerospace Systems Design Laboratory, Daniel Guggenheim School of Aerospace Engineering, Senior Member AIAA.

[4] Boeing Professor of Advanced Aerospace Systems Analysis and Director, Aerospace Systems Design Laboratory, Daniel Guggenheim School of Aerospace Engineering, Associate Fellow AIAA.

I. Introduction

THERE is an ongoing affordability paradigm shift in industry and academia which seeks to change the way in which complex systems are designed. Due to the competitive nature of the market, design has shifted from design for performance to design for overall capability. This has led to a need for forecasting the economic viability of a system with a high probability of success. In the case of the structural design of airframes, it is desirable not only to estimate the structural weight of concepts, but also the cost of manufacturing these concepts. This is especially the case with advanced structural materials such as advanced composites. Often, airframe weight cannot be reliably used to predict the manufacturing cost of these structures for reasons ranging from lack of statistical data to the dependence of manufacturing cost on other variables such as part count.

To produce structures that utilize such materials, there tend to be significantly higher manufacturing costs relative to structures made from traditional materials such as aluminum alloys. This is due to higher material and tooling costs, as well as longer manufacturing times. Moreover, there are various methods of manufacturing, raw material forms etc. available to aircraft companies all with varying costs. This implies that there needs to be careful consideration of the manufacturing costs associated with producing concepts that utilize these materials at the preliminary design level. Such considerations may help designers to better adhere to budgetary constraints by allowing them to quickly assess the impacts of making permutations to design variables, and then possibly trade structural efficiency in order to obtain a more affordable design.

Furthermore, in the earlier stages of design, it is desirable to explore a variety of shapes and designs of the structural concepts. This imposes the requirement of parametric models that seamlessly incorporate such changes and transfer the relevant data throughout the constituent modules.

This paper addresses the creation of a parametric modeling and simulation environment which uses high level geometric, performance, and structural design variables as inputs in order to facilitate a fully integrated structural analysis, optimization, and manufacturing cost assessment of the wing-box of a sub-sonic fighter aircraft. The wing-box is used as a proof of concept because it provides a variety of structural shapes, requiring various manufacturing processes and tooling. This environment is then used to provide the requisite data for the creation of surrogate models of wing-box weight and its associated manufacturing cost as functions of the aforementioned variables. These surrogate models are then coupled with a simple multi-objective genetic algorithm to provide a family of non-dominated solutions which can be used to facilitate the previously mentioned trade between structural efficiency and affordability of the concepts being explored. A handful of designs can then be chosen subjectively for further exploration and refinement, in order to gain even more accurate estimates of weight and manufacturing cost.

II. Methodology

The modeling and simulation environment that was used for this study is presented in Figure 1. All modules except for the External Loads and Structural-Manufacturing Data Translator modules utilize commercially available software that are commonly used in industry for the structural design and manufacturing cost estimation of complex systems (airplanes, launch vehicles, ships etc). They are integrated via Phoenix Ingration's Model Center. This allows for the seamless transfer of data amongst the modules in a purely automated manner. This is in an effort to carry out a fully automated linear static analysis of the wing-box model. The wing design and the constituent modules are described in the sub-sections that follow.
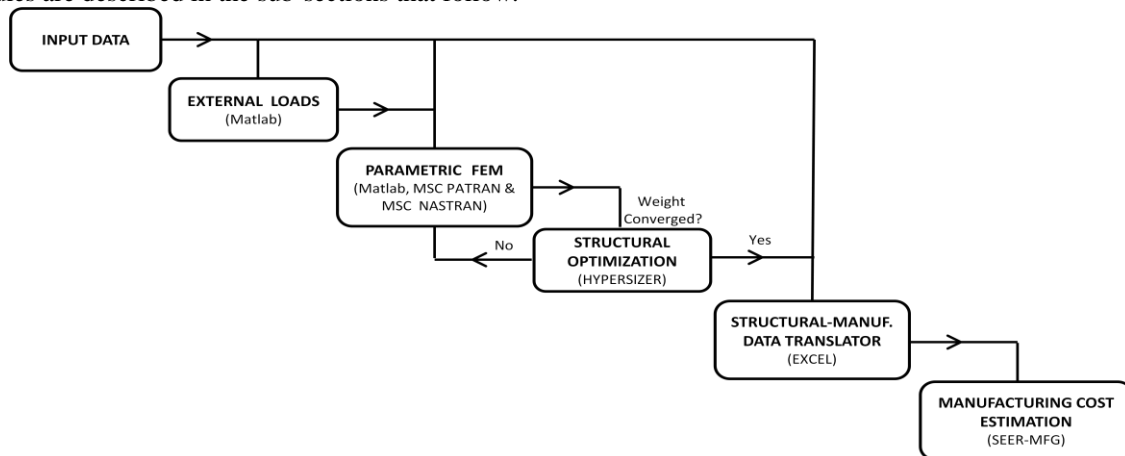

Figure 1.   Modeling and Simulation Environment

2
American Institute of Aeronautics and Astronautics

A. Wing-Box Design and Parameterization

The wing-box that is utilized in this paper is a two spar, multi-rib design based on the wing-box that was investigated in Ref. 1. It is an advanced design that features the exclusive use of graphite-epoxy composites as the primary structural material (Figure 2a). All of the features of this wing-box were retained for the current analysis except for the rib design. The original design featured a rib with integral undulations in the web as opposed to discrete stiffeners. The alternative rib design (Figure 2b) features a corrugated web with the upper and lower intercostal/shear-tie combination joined to the web by a combination of pastebonding and damage arrestment fasteners. It is considered that such a wing-box is ideal for investigation because it aids in identifying the economic impact of manufacturing diverse structural parts from advanced materials.

a)   b)
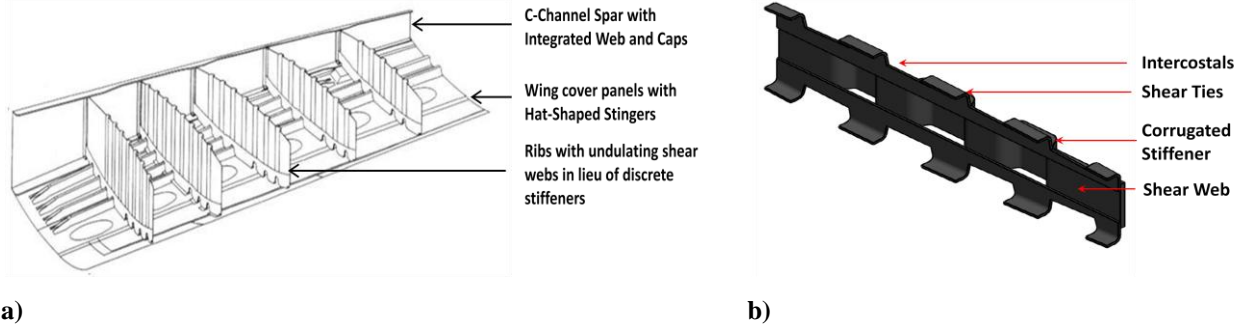
Figure 2a) Wing-box investigated in Ref. 1 b) Alternative rib investigated in the current study.

Over the years, major aircraft companies have adhered to certain design practices in the design of aircraft components and sub-assemblies. As a result, there is a plethora of guidelines available for parameterizing the structural model. An example is the position of the forward and aft spars along the wing chord in order to provide sufficient space for the auxiliary services and high-lift devices present within and on the wing. Many similar design practices pertaining to the positioning of major components[2-3] have been applied to the geometric model in order to facilitate the translation of the planform variables to resulting wing-box geometries. However, certain key variables that affect structural weight and manufacturing costs have not been frozen, but were allowed to be optimized. These include: rib spacing; stringer spacing; rib and spar stiffener spacing; and all part thicknesses.

The external shape of the overall wing was modeled after that of the F-86F aircraft. This aircraft was chosen due to the availabililty of non-proprietary data. It featured a simple trapezoidal wing with the NACA-0012 and NACA-0011 airfoils at the root and the tip respectively. The internal layout of the ribs was simplified into two regions of independent rib spacing with a transition point located at the 60% point outboard along the span. This simplified wing-box is shown in Figure 3.
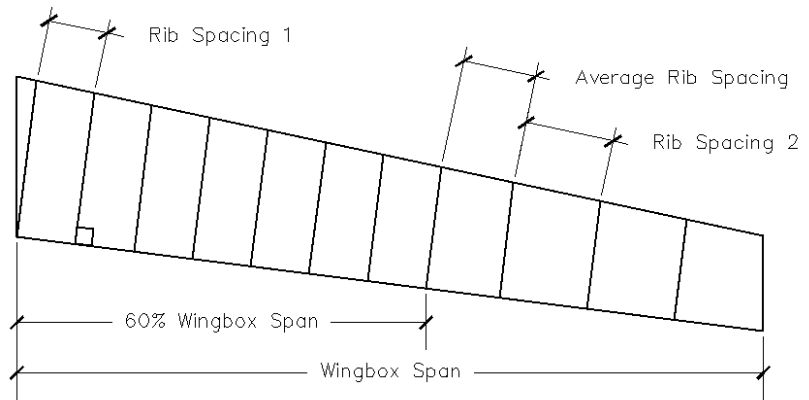
Figure 3. Simiplified wing-box model

B. External Loads

In order to simplify the scope of the linear static analysis of the wing-box, flexural and torsional aeroelastic effects were not taken into consideration. Additionally, fatigue in the wing box design was not taken into consideration, nor are any concentrated torques due to moments generated by high-lift devices and control surfaces.

The limiting load case chosen for the wing box is a 5g symmetric pull-up maneuver. For the calculation of the take off gross weight (TOGW), Fuel Weight (FW), and Wing Empty Weight (WW), pre-existing surrogate models for the F-86F that are functions of the wing planform and performance variables were utilized. The WW surrogate model was scaled by a factor obtained from Ref. 4 to allow for an approximate weight reduction in an attempt to

capture the use of advanced composites as the structural material. The resulting WW is applied along the span as a trapezoidal distribution whose local magnitude is proportional to the local chord.

For a wing that possesses aerodynamic and/ or geometric twist, the distributed lift load can be separated into two components: *basic* and *additional* lift. The former corresponds to the lift present on the wing planform at its zero-lift angle of attack, whereas the latter corresponds to the lift distribution that is added to the basic lift distribution for angles of attack beyond that corresponding to zero lift. Figure 4 shows the basic lift distribution for a wing that possesses geometric washout. The inboard portion of the wing produces positive lift whereas the outboard portion produces negative lift. The result is zero equipollent lift load.
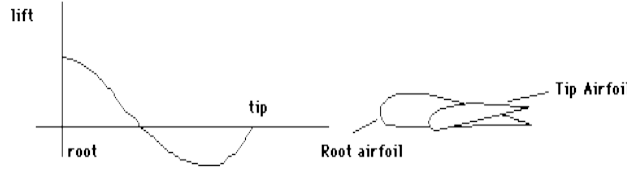
Figure 4. Basic lift load distribution on a wing possessing wash-out

According to Ref. 5, the normalized basic lift distribution for wings with symmetrical twist about the aircraft centerline may be estimated by Eq. (1):

$$\frac{C_{lb}c}{b} \approx \frac{\varepsilon - \bar{\varepsilon}}{1 + \frac{360a}{\pi^2 A}}\left(\frac{C_{la1}c}{b}a\right) \tag{1}$$

Where:

$$\bar{\varepsilon} = A \int_{-1}^{1} \varepsilon \frac{C_{la1}c}{b} d\left(\frac{2y}{b}\right) \tag{2}$$

$$a = \frac{A}{\frac{A\vartheta}{cos\Lambda}+2}\left(\frac{\pi^2}{90}\right) \tag{3}$$

$$\vartheta = \sqrt{1 + \frac{4cos^2\Lambda}{A^2}} \tag{4}$$

The C_{la1} distribution was estimated from curves presented in Ref. 6. These curves were created using the Weissinger method as applied to various taper ratios, aspect ratios and sweeps at several span-wise stations. The Weissinger method is based on the lifting line theory, but has modifications that allow for wing taper, wing sweep, and low aspect ratios. As presented in Ref. 6, the results of this method have shown reasonable agreement with wind-tunnel test data for several wing planforms. Both of these normalized distributions, when multiplied by the lift required and summed, give the spanwise lift distributions at the locus of the aerodynamic center of the airfoils along the wing.

To simulate the fuel stored in the wing, the inertia of the fuel due to the maneuver is applied to the lower wing skin as a pressure load. Due to the wing's dihedral, the local magnitude of this fuel pressure is proportional to the depth below the most outboard rib that bounds the fuel tank. The resultant lift load and weight inertia as applied to the locus of the aerodynamic centers and approximate sectional center of gravity respectively along the wing span are shown in Figure 5a. The resulting distributions are discretized and applied as equipollent loads and moments at each rib at its intersection with the center of gravity locus (Figure 5b). Of special note is that the airfoils for the chosen planform have negligible coefficient of moment for an exhaustive number of flight conditions and angle of attacks as presented in Ref. 7. This explains the absence of the pitching moment distribution that typically accompanies the distributed spanwise load along the locus of the aerodynamic center along the wing in Figure 5a.

a)   b)
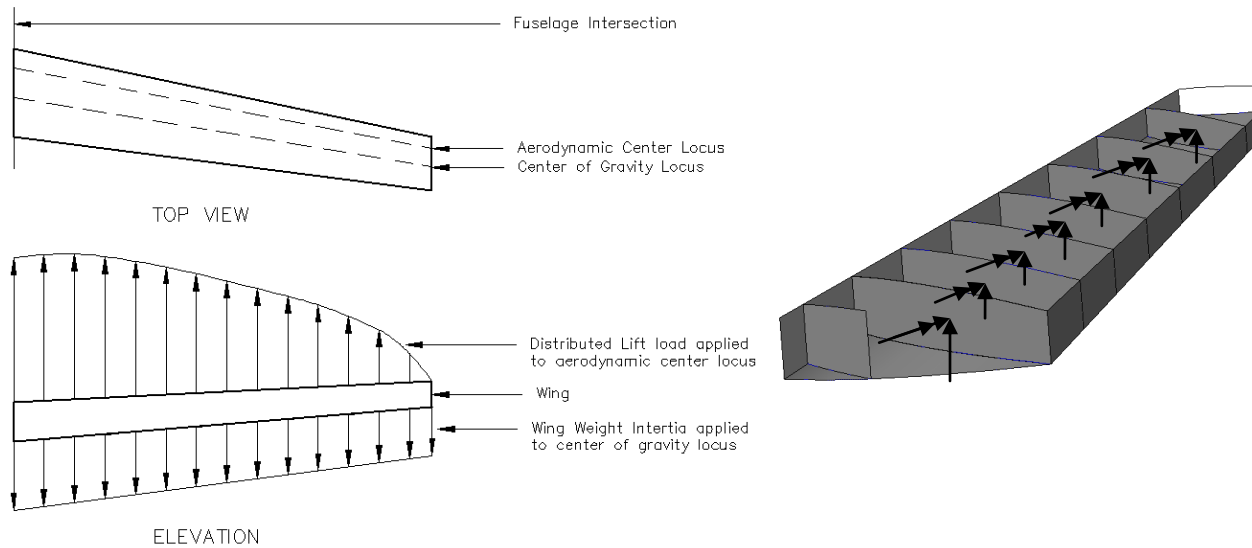
Figure 5a). Lift and weight distributions applied to the entire wing. 5b) Discretized loads and moments applied to each rib at the approximate wing center of gravity locus

C. Finite Element Model Parameterization and Structural Analysis

For the purpose of structural analysis, the finite element method was chosen. Reference 8 presents two modeling strategies for the purpose of creating finite element models (FEM) for structures. These are the "super-modeling" and "sub-modeling" strategies. The former typically utilizes fine meshes in an effort to facilitate continuum analysis in solid mechanics problems. In the latter case coarser meshes consisting of lower order elements are typically employed with mesh refinement taking place in the close vicinity of the most significant stress risers. Many of the structural components present in aerospace structures align with the latter category (Ref. 8); therefore, sub-modeling was chosen for this analysis. Additionally, for the initial sizing and global optimization of structures, coarse meshes are typically utilized. This modeling strategy as applied to the wing-box is shown in Figure 6.

a)   b)
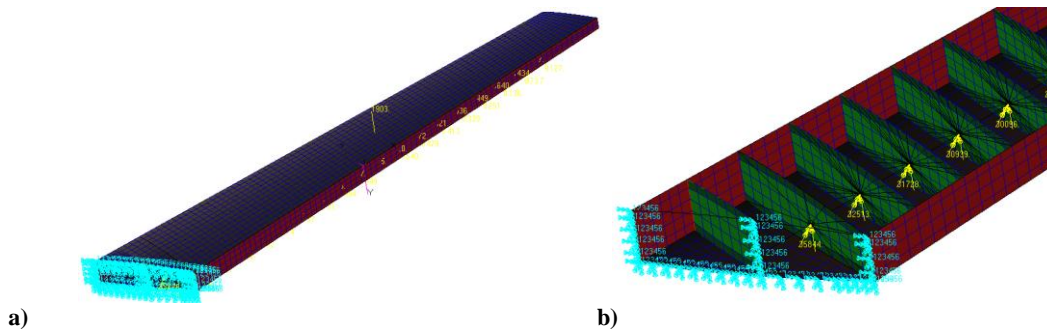
Figure 6a) Wing-box finite element model 6b) Resulting lift loads and torques applied to each RBE3 element located in close proximity to the ribs

In addition to the sub-modeling strategy, the equivalent stiffness method is used for all stiffened panels contained within the model. The equivalent stiffness method uses the classical lamination theory to facilitate the convenient analysis of a skin-stringer panel as an equivalent orthotropic sheet. This is done by "smearing" the stiffeners into this equivalent orthotropic sheet and providing a constitutive relationship between the cross-sectional loads (N_x, N_y, N_{xy}) and moments (M_x, M_y, M_{xy}) for each panel, to associated cross-sectional strains (ε_x, ε_y, ε_{xy}) and curvatures (κ_x, κ_y, κ_{xy}). This constitutive relationship takes the form of the [A,B,D] stiffness matrix as shown in Eq. (5).

$$\begin{Bmatrix} Nx \\ Ny \\ Nxy \\ Mx \\ My \\ Mxy \end{Bmatrix} = \begin{bmatrix} A & B \\ B & D \end{bmatrix} \begin{Bmatrix} \varepsilon x \\ \varepsilon y \\ \varepsilon xy \\ \kappa x \\ \kappa y \\ \kappa xy \end{Bmatrix} \qquad (5)$$

This constitutive relationship is used to provide equivalent shell properties for panels within the FEM. This formulation has been shown to give reasonable agreement with experimental results as shown in Ref. 9. This approach is advantageous to designers because relatively simple finite element models can be created in order to determine the internal loads present for a given exernal loading case. The actual panel and beam cross-sectional dimensions can then be optimized offline with subsequent iterative updates of the FEM's shell properties until the weight of the model converges.

For the parameterization of the finite element model, the Patran Command Language (PCL) was utilized. The PCL is a high level block structured programming language integral to the finite element pre/post − processing software MSC Patran. This language provides the capability of creating and analyzing finite element models with similar functionality to that provided by Patran's Graphical User Interface (GUI). With the aid of the aforementioned design practices, an algorithm that translates the geometric and structural variable inputs to the representative finite element models was written in MATLAB. Each unique model that results provides representative component and initial internal loads data for the subsequent structural optimization process.

D. Structural Optimization

Hypersizer, a structural optimization software, was used for the task of optimizing the weight of each wing-box model. Hypersizer supports the previously mentioned equivalent stiffness method by providing many panel concepts which are optimized offline to provide the composite laminate ply percentages via effective laminates, cross-sectional dimensions, and the stiffener spacing required for the lightest structurally admissible design for a particular load scenario. Hypersizer also contains many failure analyses and geometry checks to ensure that the designs are not only structurally admissible, but that they also meet certain design rules of thumb that are typically observed in aircraft structural design. Figure 7 shows the hat-stringer stiffened panel employed for the wing-covers of the design. The failure analyses in Hypersizer check not only for material strength but also for the more intricate failures such as the buckling of the entire panel, the local buckling of the effective and unsupported strips of wing-skin, and the local buckling of the stringer web and bottom crown.
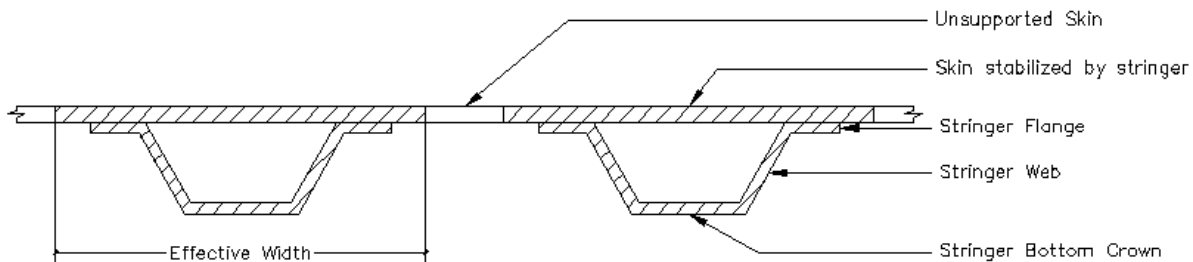
Figure 7. Section of a hat-stringer stiffened panel

It should be noted at this stage that only the cross-sectional dimensions of the beams and panels are optimized. Rib spacing, which is a critical decision variable with respect to wing-box weight, will be optimized at a later stage in the present development.

Figure 1 shows a feedback loop between the structural optimization and the FEM modules; this is necessary in order to provide an update of the shell properties within the FEM model to reflect the optimized dimensions and material data for the previous iteration of the structural optimization. The feed forward loop between these modules provides updated internal forces associated with the updated shell properties. This iterative loop continues until there is a weight convergence of the model. The resulting optimized component data are then passed to the Structural to Manufacturing Data Translator module which serves as a means of translating the data into a manageable form for the manufacturing cost estimation model.

E. Manufacturing Cost Estimation

Innovative designs enabled by composite materials and advanced manufacturing processes has led to higher design freedom and reduced weight, but typically increased manufacturing cost (Ref. 10). Design for manufacturing has shown that there are other key cost drivers beyond weight, such as part and fastener count (Ref. 11). Further, eighty percent of costs are locked at the end of the preliminary design level. As a result, engineers should no longer take a strictly weight based approach to manufacturing cost estimation[12,13]. Preliminary level variables need to be taken into account to accurately estimate cost and conduct trades.

In order to assess manufacturing costs at a preliminary design level, SEER-MFG by Galorath, an empirical, process-based cost tool was utilized. SEER-MFG contains relevant, current aerospace data, which were taken off of ITAR restriction in 2007. SEER-MFG features a large breadth and depth of manufacturing processes that are production plan configurable. The preliminary level of design detail captured in SEER-MFG is shown in Figure 8 for a corrugated rib. Inputs for the corrugated rib include number, depth, and angle of corrugations.

A detailed production plan was defined within SEER-MFG for the ribs, spars, stringers, skins, and assembly (Figure 9). The corrugated rib web pre-form was hand-layed, Vacuum assisted Resin Transfer Molding (VaRTM) cured, and paste-bonded to similarly manufactured intercostals and shear ties. This sub-assembly was then paste-bonded to the spar joints with the subsequent addition of auxiliary damage arrestment fasteners for fail-safe joints. Hexcel IM7 carbon fiber and CYCOM 823 RT resin were chosen for their handling, structural properties, and compatibility with VaRTM. It is important to specify the process at this level, since there are many manufacturing step alternatives and associated costs for a given part.
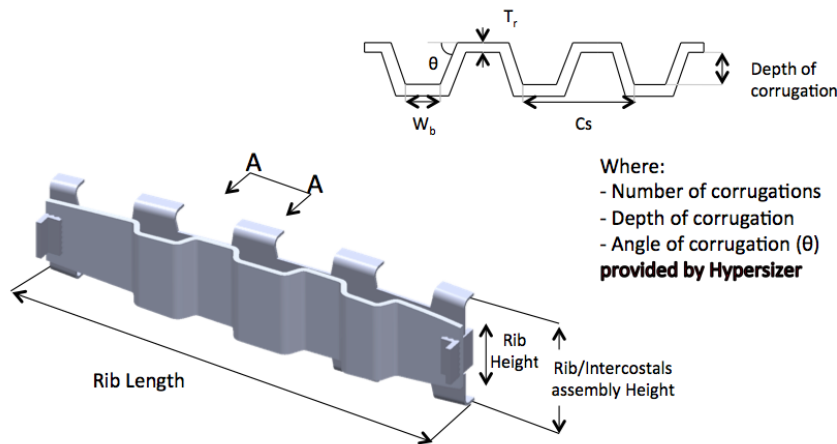
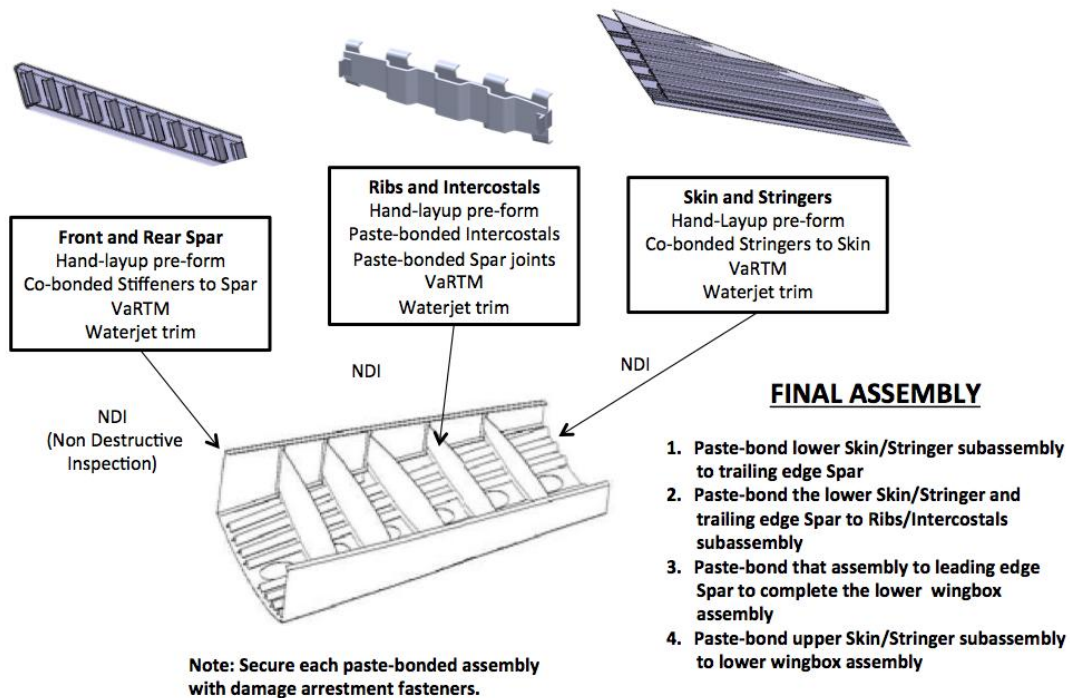
Figure 8: Rib dimension data fed to SEER-MFG

Engineering variables, such as part dimensions, ply tables, and part count, are extracted from the structural optimization tool using a structural data translator, and then fed into SEER-MFG which calculates the 100th unit cost using an 85% learning curve. The 100th unit cost includes labor, material, and tooling cost amortized over the 100 units.

F. Structural Data Translator

There is a gap between the preliminary level data that Hypersizer provides and that which SEER-MFG needs. In order to fill this gap, a structural data translator was developed using *Microsoft Excel Visual Basic for Applications (VBA)*. The translator applies industry common practices or "rules of thumb" to the optimal structure to derive manufacturing input variables, such as fastener count and join length, in order to bridge the gap between Hypersizer and SEER-MFG. For example, a part's length, fastener size, and typical industry fastener spacing were used to calculate total number of fasteners (Ref. 13).

In addition to translating the structural outputs into manufacturing variables, additional manufacturing constraints were applied to the optimized structure in order to appropriately reflect cost. For example, the orientation of plies were tailored to the load path resulting in optimal thicknesses and reduced weight in the Hypersizer model. The structural data translator takes Hypersizer's output and applies ply continuity logic to obtain a fitting ply table.

This is important because ply continuity reduces manufacturing cost and stress concentration at the interfaces between adjacent panels while increasing overall structural integrity (Ref. 14).

Front and Rear Spar
Hand-layup pre-form
Co-bonded Stiffeners to Spar
VaRTM
Waterjet trim

Ribs and Intercostals
Hand-layup pre-form
Paste-bonded Intercostals
Paste-bonded Spar joints
VaRTM
Waterjet trim

Skin and Stringers
Hand-Layup pre-form
Co-bonded Stringers to Skin
VaRTM
Waterjet trim

NDI

NDI

NDI
(Non Destructive Inspection)

FINAL ASSEMBLY

1. Paste-bond lower Skin/Stringer subassembly to trailing edge Spar
2. Paste-bond the lower Skin/Stringer and trailing edge Spar to Ribs/Intercostals subassembly
3. Paste-bond that assembly to leading edge Spar to complete the lower wingbox assembly
4. Paste-bond upper Skin/Stringer subassembly to lower wingbox assembly

Note: Secure each paste-bonded assembly with damage arrestment fasteners.

Figure 9.   Manufacturing processes definitions for the wing-box

An example of the data translation process is the wing box skin below. In Hypersizer, a local optimization of the ply table for each panel was performed (Figure 10a), based on the local edge loads and moments calculated for that panel. The individual ply tables were then grouped into seven panels and then translated to seven overlapping ply drops from the wing tip to the root (Figure 10 b-c). The reason the skins were grouped into seven larger structural panels was to simplify the interface between Hypersizer and SEER-MFG and better reflect manufacturing costs. The number of plies in each orientation for these larger panels was determined by the maximum number of plies in that particular orientation amongst the constituent panels. A guide with 100% coverage of the wing box skin was then defined at the wing tip by the ply table of the first and thinnest panel. The additional drops were evaluated as a difference between the related panel and the guide. This guide-based approach ensures complete blending, while producing the appropriate manufacturing lay-up costs (Ref. 15).

a)   b)   c)
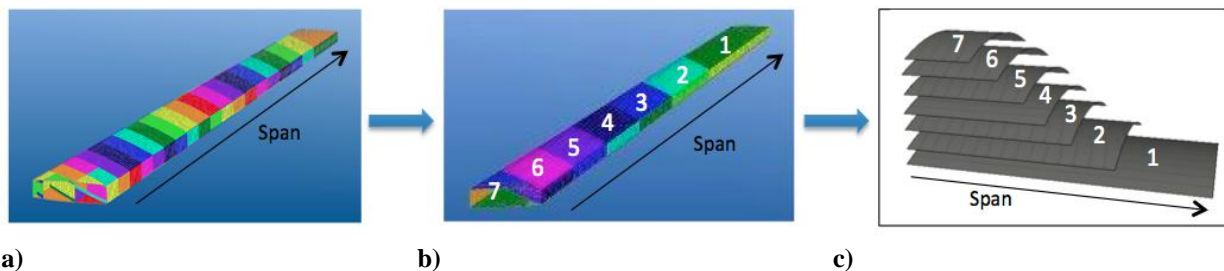
Figure 10. Ply table data translation. a) Original structural panel distribution. b) New seven panel distribution. c) Drops distribution to ensure blending.

American Institute of Aeronautics and Astronautics

In order to validate the process, the seven ply-drops method was compared to the original structural panel distribution and a maximum, constant thickness approach for the wing-box baseline. The results are shown in Table 1. The seven ply-drops method decreased the set-up hours and material cost per unit from the original panel method. The maximum, constant thickness method further reduced set up hours per unit but was extremely expensive in terms of material cost and ply placement direct hour per unit. After socializing the results with subject matter experts, the seven ply-drops method was determined to be a less complex and a preferable manufacturing definition of the component (Ref 16). The magnitude and trends were deemed to be more practical.

Table 1. Comparison between different drop methodologies

	REFERENCE: Original Structural Panels from Hypersizer	OPTION 1: Seven Ply-Drops Method	OPTION 2: Maximum Constant Thickness Method
Labor Cost per Unit	$	-3.65%	-2.73%
Material Cost per Unit	$	-0.74%	82.89%
Total Recurring Fab Cost per Unit	$	-2.16%	41.13%
Hand Layup Set-Up Hours per Unit	17.2	-37.98%	-58.44%
Ply Placement Direct Hours per Unit	18.8	5.19%	77.61%
Total Direct Hours per Unit	33.6	7.59%	25.79%

G. Surrogate Models

As is often the case with simulations, there is a significant computational cost associated with running each unique wing-box analysis, especially for those designs that feature many structural panels. It is for this reason that surrogate models were created. A surrogate model is a statistical regression that provides a functional approximation to an often more complicated simulation or experiement. By using carefully selected data points in the form of a design of experiments, neural network surrogate models were trained for wing-box weight and average unit cost as functions of the planform variables, mission flight range, and both independent rib spacings. These surrogate models require significantly less computational time, but with the compromise of reduced accuracy. Care must be taken in ensuring that surrogate models are used within the design variable ranges for which they are created. If used for extrapolation, extremely erroneous results may occur.

II. Strategy for Rib Spacing Optimization

A. Rib Spacing Optimization

The problem of rib spacing optimization is visually represented in Figure 11. The traditional approach from a structural optimization standpoint is to find the value(s) of rib spacing(s) required to produce the optimum combination of the weight of the wing covers and aggregate rib weight[3,17,18].

However, consider the sensitivity plot shown in Figure 12. It shows the effect of the planform variables, mission flight range, and rib spacings on the average unit cost of the wing-box for the ranges specified in Table 2. Notice the significant impact that the inboard rib spacing has on the average unit cost of the wing-box. This is due to the significant expense of producing each rib, which is mainly due to:

(i)   Labor intensive manufacturing process
(ii)   Tooling cost penalty incurred for introducing each unique rib (Unique due to wing taper)
(iii)   Fastener and assembly costs for each additional rib

This observation implies that, provided all the other variables are held constant, fewer ribs (hence larger rib spacing) leads to a lower unit cost for a particular wing-box. The large expenses associated with manufacturing ribs is not atypical in wing-box production. Therefore, when affordability comes into consideration, both structural efficiency and manufacturing cost need to be simultaneously considered in the rib spacing optimization problem.
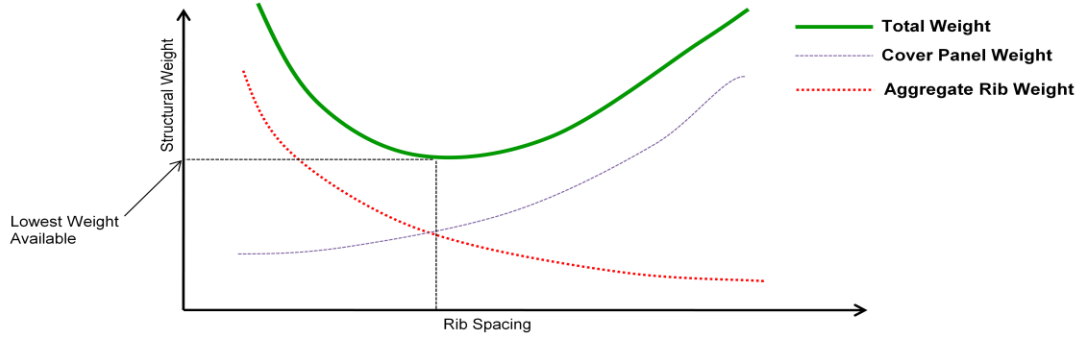
Figure 11. Notional plot showing the behavior of wing-box weight with varying rib spacing
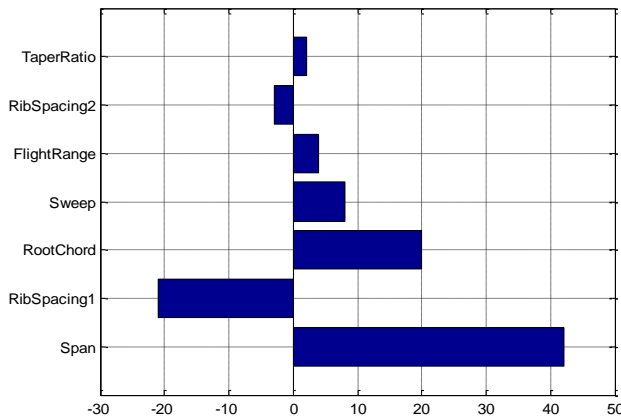

Figure 12. Tornado plot showing the sensitivity of wing-box unit cost to the design variables

Table 2. Ranges for the design variables

Variable	Lower Limit	Upper Limit
Taper Ratio	0.36	0.67
RibSpacing2 (in)	8	40
FlightRange (nm)	220	1038
Sweep (deg)	24	45
RootChord (ft)	7.1	16.19
RibSpacing1 (in)	8	40
Total Wing Span (ft)	27.1	50.1

B. Multi-Objective Genetic Algorithm

In order to solve this multi-objective problem, wherein it is desirable to simultaneously minimize both the wing-box weight and average unit cost, a multi-objective genetic algorithm was utilized. The genetic algorithm is a heuristic optimization algorithm that is based on the theory of evolution, particularly natural selection. This theory proposes that organisms that possess greater fitness have a stronger likelihood of surviving and hence passing on their genes to the next generation by means of reproduction. The simple, multi-objective form of this algorithm has the following steps:

(i)   The generation (often random) of an initial population within a design space.
(ii) An iterative ranking process: the non-dominated candidates within the population are given the highest rank and then removed from the population. The non-dominated solutions in the remaining population are similarly ranked, but at a lower level and then removed. This continues until all the members of the population are ranked.
(iii) Reproduction via cross-over and mutation: Two members of the population are chosen randomly. Higher probabilities of selection are placed on those members of the population with greater fitness/ higher rank. Information from these two "parents" are passed onto the two resulting "children" by the process of crossover. This process is analagous to sexual reproduction. Parts of these children may change at random, depending on the mutation probability in the process of mutation. This is in an effort to encourage diversity among the population members.
(iv) Step iii continues until a new population is generated
(v)   Steps ii – iv are continued until the algorithm converges to the Pareto optimum set in the design space

10
American Institute of Aeronautics and Astronautics

For further information on the multi-objective genetic algorithm (MOGA), please see Ref. 19. The resulting Pareto optimum set contains a subset of the candidates in the design space with the best combination of objective values, in this case wing-box weight and average unit cost. The process is illustrated with the following case study.

III. Case Study

A fixed wing-box planform was investigated in this case studyS. The reason for this is due to the fact that the planform variables cannot be optimized without considering the effects on other disciplines such as aerodynamics. For simplicity, the flight range was also fixed. These values are shown in Table 3. The optimization problem with the introduction of side constraints on the rib-spacings is stated formally as follows:

$$Minimize\ WBW(RS1, RS2)$$
$$Minimize\ AUC(RS1, RS2)$$

$$Subject\ to:$$
$$8”≤ RS1≤ 40”\ and\ 8”≤ RS2≤ 40”$$

Where:

WBW: Wing-box Weight
AUC: Average Unit Cost
RS1, RS2:   Rib spacing in the inboard and outboard sections of the wing, respectively

Figure 13 shows contour plots of the design space for wing box weight and average unit cost that were created using the surrogate models. From Figure 13a one can see that the behavior for the wing-box weight is convex with a clear global optimum occurring within the domain. This behavior is similar to that presented in Figure 11. This is due to the trade in wing-cover and aggregate rib weight for increasing rib spacing. As rib spacing is increased, the buckling span for each of the compression panels bounded by the ribs increases. This results in an increase in the material – hence weight – required for structural admissibility of these panels. At the same time there is a reduction in the number of ribs for increasing rib spacing. The reduction in aggregate rib weight outweighs the increase in wing-cover weight until the global minimum occurs. Thereafter, the behavior reverses and the increase in aggregate wing cover weight outweighs that of the ribs leading to an overall increase in wing-box weight.

With respect to the average unit cost of the wing-box Figure 13b, as the rib spacing is increased- hence number of ribs is decreased- there is a reduction in this objective. The global optimum appears to be towards the edge of the design space where the inboard rib spacing is maximum and the outboard rib spacing is in the upper half of its range. This is in keeping with the previously shown sensitivity plot (Figure 12) which shows that there is a strong correlation between the increase of rib spacing and the reduction of average unit wing-box cost.


a)   **b)**
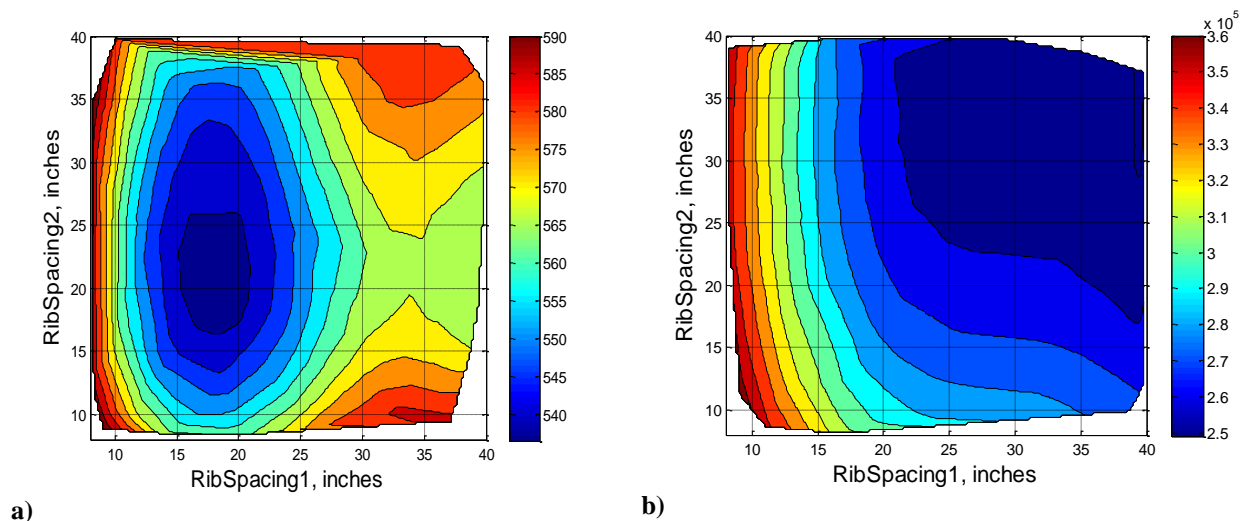
Figure 13a) Contour plot of wing-box weight (lbs) vs. rib spacings (inches) b) Contour plot of average unit cost (FY$2010) vs. rib spacings (inches)

For this case study, MATLAB's built-in MOGA function was used. Two points must be noted with regards to the usage of the MOGA for this case study. Firstly, the initial population was generated randomly so as not to favor either objective as the algorithm proceeded. Secondly, and similarly, both objectives are equally weighted because the assumption is made that the preferences between the objectives are not known a priori, leaving subjective selection of candidates until after the process is completed.

An initial population consisting of 200 members was generated for the MOGA. The number of generations was set to 1000, and the cross-over probability was set to 80%. The mutation probability was governed by MATLAB's default settings which assigns a probability of mutation to each entry in the parent vector as selected from a Gaussian distribution. This feature is dynamic in that the amount of mutation, which is proportional to the standard deviation of the distribution, decreases with each new generation. The initial population overlaid on the contour plot of both objectives is shown in Figure 14. It can be seen here that there is good coverage of the design space. The algorithm was then executed, and it converged in 325 generations. The convergence criterion was that the average change in the spread of the Pareto solutions was below the tolerance. The final Pareto frontier designs are shown on the contour plot of each objective in Figure 15. The final set of solutions has some of its members in the optimum region for each objective in its design space. Figure 16 shows the Pareto Front plotted in the objective space. It can be seen that the two objectives are adversely related meaning that there has to be a trade off between weight and cost when a design(s) is to be selected. In order to facilitate this selection, the Technique for Order Preference by Similarity to Ideal Solution (TOPSIS) method was used. This method is a multi-criteria decision making technique in which, based on preferences expressed, an ideal solution is generated. The solution that is closest to this solution in terms of Euclidian distance is selected. Referece 20 provides further information on TOPSIS.
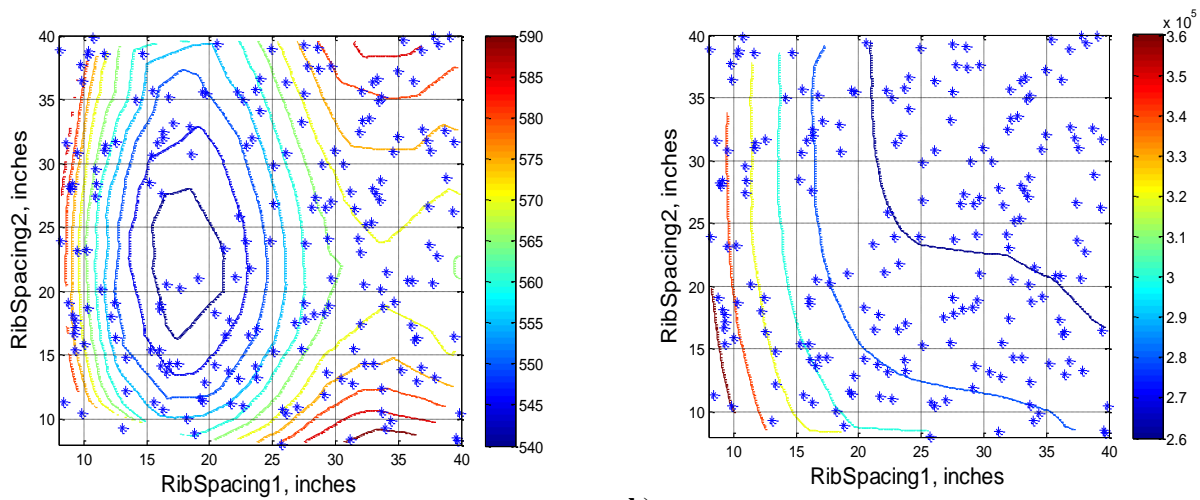
a)

Figure 14a)   Overlay of initial population on wing-box weight (lbs) contours. b) Overlay of initial population on average unit cost (FY$2010) contours
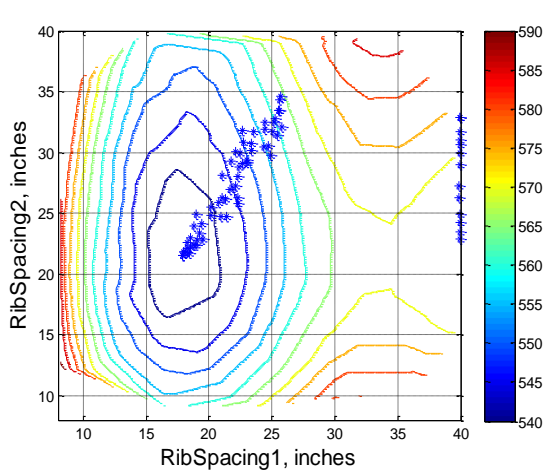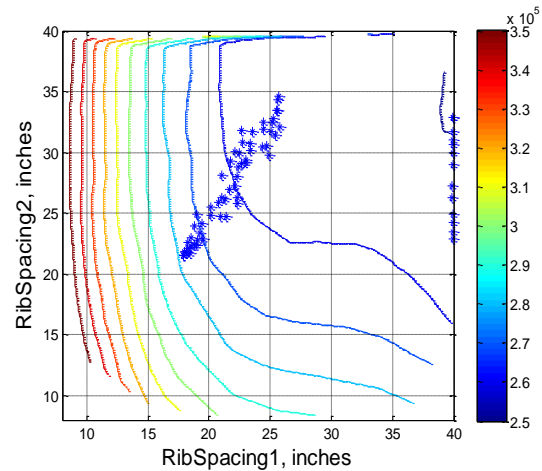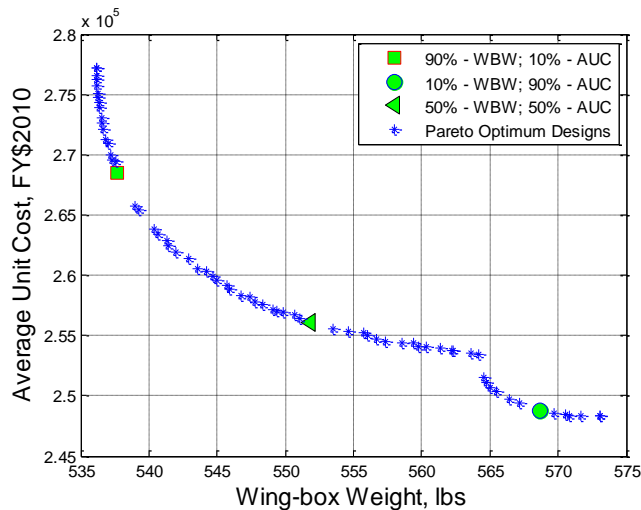
a)   **b)**

Figure 15a)   Overlay of the Pareto optimum solutions on wing-box weight (lbs) contours. b) Overlay of Pareto optimum solutions on average unit cost (FY$2010) contours

Figure 16. Pareto optimum solutions in the objective space

Table 3. Variable settings for the case study

Total Wing Span (ft)	50.0
Root Chord (ft)	16.0
Sweep (deg)	45.0
Taper Ratio	0.40
Flight Range (nm)	1038

A few scenarios involving different objective preferences are shown in Table 4. The preference/weighting for each objective is expressed as a percentage. Please see Figure 16 for further reference.

Table 4.   Selected designs based on preferences expressed between the two objectives

WBW Preference(%)	AUC Preference (%)	WBW (lbs)	AUC (FY$2010)	Percent > Min. Weight (%)	Percent > Min. Cost (%)
90	10	537.65	268,539	0.28	8.15
10	90	568.70	248,718	6.07	0.17
50	50	551.80	256,100	2.92	3.14

IV. Conclusion

A. Case study conclusions

For the purposes of structural analysis, optimization, and manufacturing cost assessment of aircraft structures, several preliminary & detailed design level methods and software packages are available. The methods can be used to make computer programs and the software packages can be automated to facilitate the incorporation of higher fidelity methods into the earlier stages of design in order to reduce uncertainty. This approach was applied to a multi-rib wing-box that featured the exclusive use of carbon fiber – epoxy resin composites. While many of the structural variables corresponding to the dimensions of the structure were optimized by the suite of methods and tools, rib spacing was shown to not only have an impact on weight, but also on manufacturing cost. This prompted the use of multi-attribute optimization and selection techniques in order to select a subjective optimum design. For the case study, single point designs were selected based on preferences expressed; however, it is advised that these preferences be given ranges so that a group of designs may be selected. This is due to the fact that many sources of uncertainty still remain ranging from simplifications in the analyses to factors that were not taken into consideration. This handful of designs can be assessed with even higher levels of detail in order to attain even more accurate estimates of structural weight and cost. However, the steps up to this point have allowed the designer to explore the design space and then collapse it to the region of interest.

B. Generalization of approach

A similar process to that carried out for the wing-box can be used for other assemblies in the airframe with the following general approach:

- **Problem definition:** The problem definition involves various influencing factors, such as: interests/needs; available resources and time; existing understanding of the problem, etc. These factors play an important role in defining scope of work, level of fidelity, and assumptions.
- **Parametric, preliminary structural and costing modeling and simulation (M&S) environment:** Based on the problem definition, a set of commercial and/or in-house tools/methods can be selected to assemble a baseline modeling and simulation flow. Upon validation of the baseline, an automated, parametric environment can then be built. Either commercially available intergration tools (such as ModelCenter and iSight) or customized scripts can be used to develop such an integrated parametric environment. Utilizing the extensive aircraft design practices that are available, the parametric models can be used to translate high level variables into resulting structural designs.

  Tools that facilitate the integration of structures and manufacturing cost estimation are typically not readily available and need to be built. This involves the usage of industry common practices in order to bridge the gap between the output of structural optimization tools and manufacturing cost estimation models.
- **Surrogate modeling:** The M&S environments are typically computationally expensive; therefore, it is often convenient to use surrogate models for the purpose of providing objective values. The requisite data for the surrogate models can be obtained by carrying out a design of experiments on the M&S environment. Once validated for the desired level of accuracy, the surrogate models provide a more computationally expedient means of calculating objective values for the design variable ranges of interest.
- **Multi-objective optimization:** Associated with the creation of surrogate models via statistical software packages such as JMP from SAS, is the capability of generating sensitivity plots similar to the tornado plot shown in Figure 12. These sensitivity plots can be used to identify the main weight and manufacturing cost variability drivers in structural design as was done in the rib spacing optimization. These design variables can then be optimized in the face of adversely related objectives by means of utilizing multi-objective optimization methods. Candidates can then be selected subjectively via multi-objective selection techniques.

Acknowledgments

References

[1]Toi, Y., Harada, A., Tanaka, S., Amaoka, K., and Kikukawa, H. "Development of affordable composite wing structure," *Advanced Composite Material*, Vol. 12, No. 4, 13 May. 2003, pp. 321–329.

[2]Sensmeier, M D.. and Samareh, J.A.: "A Study of Vehicle Structural Layouts in Post-WWII Aircraft' NASA Rep. No. 1624 (2004)

[3]Niu, M.C.Y, *Airframe Structural Design*, 2nd ed., Hong Kong Conmilit Press Ltd., North Point, Hong Kong, 1999, Chaps. 3, Chaps. 8

[4]Raymer, D.P, *Aircraft Design: A Conceptual Approach*, 4th ed., AIAA Education Series, AIAA, Virginia, 2006, Chaps. 15, pg. 455

[5]DeYoung, J. and Harper, C.W.: 'Theoretical Symmetric Span Loading at Subsonic Speeds for Wings Having Arbitrary plan form.' NACA Rep. No. 921, (1948)

[6]Sivells, J.C.: 'An Improved Approximate Method for Calculating Lift Distributions due to Twist.' NACA TN 2282, (1951)

[7]Ladson, C.L. and Acquilla, S.H.: 'High Reynolds Number Transonic Tests of an NACA 0012 Airfoil in the Langley 0.3-Meter Transonic Cryogenic Tunnel.' NACA Technical Memorandum 100527, (1987)

[8]Morris, A. J., Taig, I.C., and Venkayya, V. B., Practical Application of Finite Element Analysis to Aircraft Structural Design, AGARD, 1986, pp : 3-1 to 3-18

[9]Wu, C.L. and Duan, S.H.: 'Buckling Behaviour of Composite Laminated Corrugated Panel with Sinusoidal Profile Part 1: Equivalent Stiffness Terms.' Aircraft Strength Research Institute of China, Xian, 710065 China (2009)

[10]P.Stickler, "Composite Materials for Commercial Transport – Issues and Future Research Direction" Proceedings of the ASC, 17th Annual Technical Conference, West Lafayette, IN, 2002

[11]Army Materials and Mechanics Research Center, "Military Handbook Design Guide for Producibility" (MIL-HDBK-727), Department of Defense, Washington, D.C., 1984

[12]Johanna M. Ceisel, Philipp Witte, Tim Car, Satya Pogaru, Dimitri N. Mavris, "A Non-Weight Based, Manufacturing Influenced Design (MInD) Methodology for Preliminary Design," 28th Congress, ICAS, Brisbane, Australia, 2012 (to be published)

[13]T. Gutowski, Henderson, R., and Shipp, C."Manufacturing Costs for Advanced Composites Aerospace Parts," SAMPE Journal, Vol. 27, No. 3, 1991, pp.37-43

[14]Liu, D., Toropov, V. V., Zhou, M., Barton, D. C., Querin, O. M., "Optimization of Blended Composite Wing Panels Using Smeared Stiffness Technique and Lamination Parameters" 51th AIAA/ASME/ASCE/AHS/ASC Structure, Structural Dynamics, and Material Conference, Orlando, Florida, 12-15 April 2010.

[15]Seresta, O., Gurdal, Z., Adams, D.B., and Watson, L.T., "Optimal Design of Composite Wing Structures with Blended Laminates," Composites Part B: Engineering, Vol. 38, 2007, pp. 469-480.

[16]Mazumdar, S. K., *Composites manufacturing: materials, product, and process engineering,* CRC Press LLC, Boca Raton, 2002, Chaps. 5.4.

[17]Richards, D.M.., "The minimum weight design of compression structures including plasticity effects," Ph.D. Dissertation, College of Aeronautics., Cranfield Initute of Technology, Cranfield, United Kingdom, 1977.

[18]Wakayama, S., Kroo, I, "Subsonic Wing Planform Design Using Multidisciplinary Optimization," *AIAA Journal of Aircraft*, Vol. 32, No. 4, AIAA, 1995,

[19]Deb, Kalyanmoy, "Multi-Objective Optimization using Evolutionary Algorithms," John Wiley & Sons, Ltd, Chichester, England, 2001.

[20]Lai, Y-J., Liu T-Y, Hwang C-L, "TOPSIS for MODM," *European Journal of Operational Research*, Vol. 76, Issue 3, 1994, pp. 486-500

[21]Berthelot, J.M., *Composite Materials: Mechanical Behavior and Structural Analysis*, 1st ed., Springer-Verlag New York, Inc., 1999, Chaps. 14

.

American Institute of Aeronautics and Astronautics